

Sharp uniform in time error estimate on a stochastic structure-preserving Lagrangian method and computation of effective diffusivity in 3D chaotic flows

Zhongjian Wang^a, Jack Xin^b, Zhiwen Zhang^{a,*}

^a*Department of Mathematics, The University of Hong Kong, Pokfulam Road, Hong Kong SAR.*

^b*Department of Mathematics, University of California at Irvine, Irvine, CA 92697, USA.*

Abstract

In this paper, we study the problem of computing the effective diffusivity for a particle moving in chaotic flows. Instead of solving a convection-diffusion type cell problem in the Eulerian formulation (arising from homogenization theory for the Fokker-Planck equation), we compute the motion of particles in the Lagrangian formulation, which is modeled by stochastic differential equations (SDEs). A robust numerical integrator based on a splitting method was proposed to solve the SDEs and a rigorous error analysis for the numerical integrator was provided using the backward error analysis (BEA) technique [29]. However, the upper bound in the error estimate is not sharp. In this paper, we propose a completely new and sharp error analysis for the numerical integrator that allows us to get rid of the exponential growth factor in our previous error estimate. Our new error analysis is based on a probabilistic approach, which interprets the solution process generated by our numerical integrator as a Markov process. By exploring the ergodicity of the solution process, we prove the convergence analysis of our method in computing the effective diffusivity over infinite time. We present numerical results to demonstrate the accuracy and efficiency of the proposed method in computing effective diffusivity for several chaotic flows, especially the Arnold-Beltrami-Childress (ABC) flow and the Kolmogorov flow in three-dimensional space.

AMS subject classification: 35B27, 37M25, 60H35, 65P10, 65M75, 76R99

Keywords: Convection-enhanced diffusion; chaotic flows; effective diffusivity; stochastic Hamiltonian systems; ergodic theory; Markov process.

1. Introduction

Diffusion enhancement in fluid advection is a fundamental problem to characterize and quantify the large-scale effective diffusion in fluid flows containing complex and turbulent streamlines, which is of great theoretical and practical importance; see [6, 7, 4, 5, 16, 19, 2, 24,

*Corresponding author

Email addresses: ariswang@connect.hku.hk (Zhongjian Wang), jxin@math.uci.edu (Jack Xin), zhangzw@hku.hk (Zhiwen Zhang)

25, 17, 31] and references therein. Its applications can be found in many physical and engineering sciences, including atmosphere science, ocean science, chemical engineering, and combustion. To study the diffusion enhancement phenomenon, one can consider a passive tracer model, which describes particle motion with zero inertia

$$\dot{X}(t) = v(X, t) + \sigma \xi(t), \quad X \in R^d, \quad (1)$$

where X is the position of the particle, $\sigma > 0$ is the molecular diffusion coefficient, and $\xi(t) \in R^d$ is a white noise or colored noise. The velocity $v(X, t)$ satisfies either the Euler or the Navier-Stokes equation. In practice, $v(X, t)$ can be modeled by a random field that mimics the energy spectra of the turbulent flow [19].

For spatial-temporal periodic velocity fields and random velocity fields with short-range correlations, the homogenization theory [3, 10, 14, 26] states that the long-time large-scale behavior of the particles is governed by a Brownian motion. More precisely, let $D^E \in R^{d \times d}$ denote the effective diffusivity matrix and $X^\epsilon(t) \equiv \epsilon X(t/\epsilon^2)$. Then, $X^\epsilon(t)$ converges in distribution to a Brownian motion $W(t)$ with covariance matrix D^E , i.e., $X^\epsilon(t) \xrightarrow{d} \sqrt{2D^E}W(t)$, as $\epsilon \rightarrow 0$. The effective diffusivity matrix D^E can be expressed in terms of particle ensemble average (Lagrangian framework) or integration of solutions to cell problems (Eulerian framework). The dependence of D^E on the velocity field of the problem is highly nontrivial. For time-independent Taylor-Green velocity field, the authors of [27] proposed a stochastic splitting method and calculated the effective diffusivity in the limit of vanishing molecular diffusion. For random velocity fields with long-range correlations, various forms of anomalous diffusion, such as super-diffusion and sub-diffusion, can be obtained for exactly solvable models (see [19] for a review). However, the long-time large-scale behavior of the particle motion is in general difficult to study analytically.

In recent work [29], we proposed a numerical integrator to compute the effective diffusivity of chaotic and stochastic flows using structure-preserving schemes. We also investigated the existence of residual diffusivity for several different velocity fields, including the time periodic cellular flows. The residual diffusivity, a special yet remarkable convection-enhanced diffusion phenomenon, refers to the non-zero and finite effective diffusivity in the limit of zero molecular diffusivity as a result of a fully chaotic mixing of the streamlines. Mathematically, we provided a rigorous error estimate for the effective diffusivity. Specifically, let D^E denote the exact effective diffusivity matrix and $\tilde{D}^{E,num}$ denote the numerical result obtained using our method (see Eq.(8)), respectively. We obtained the error estimate, $|\tilde{D}^{E,num} - D^E| \leq C\Delta t + C(T)\Delta t^2$, where the T should be greater than the diffusion time. To the best of our knowledge, this result is the first one in the literature to study the convergence on the numerical approximation of the effective diffusivity of chaotic flows, which shows that the main source of error does not depend on time. However, the prefactor $C(T)$ in the second term may grow exponentially fast, which makes the estimate not sharp.

To get an optimal error estimate, we shall develop a completely new methodology for our numerical integrator in this paper, which allows us to get rid of the exponential growth factor. Our analysis is based on a probabilistic approach. We interpret the solution process generated by our numerical integrator as a Markov process, where the transition kernel can be

constructed explicitly due to the additive noise in the passive tracer model (1). By exploring the ergodicity of the solution process, we succeed in the convergence analysis of our method and give a sharp error estimate for the numerical solution of the effective diffusivity. Most importantly, our convergence analysis reveals the ergodic structure of the solution process, so that we can compute the passive tracer model over infinite time without losing accuracy (i.e., convergence does not depend on the computational time; see Fig.3a). Finally, we present numerical experiments to demonstrate the accuracy of the proposed method in computing effective diffusivity for several typical chaotic flow problems of physical interests, including the Arnold-Beltrami-Childress (ABC) flow and the Kolmogorov flow in three-dimensional space. The phenomenon of convection-enhanced diffusion for those velocity fields will also be investigated.

Our computation of convection-enhanced diffusivity in three-dimensional chaotic flows appears to be the first in the Lagrangian framework. Alternative computation in the Eulerian framework involves singularly perturbed advection-diffusion equations whose solutions develop sharp boundary layers with unknown locations a-priori. We are aware of only [4] on ABC flows, which we recover and go beyond by two orders of magnitude of molecular diffusivity; see the numerical results in the subsection 5.2 later.

The rest of the paper is organized as follows. In Section 2, we shall review the background of the passive tracer model and the definition of the effective diffusivity tensor using the Eulerian framework and the Lagrangian framework. In Section 3, we propose our numerical integrator in computing the passive tracer model. Section 4 is the main part of this paper, where we shall provide our new error estimate based on a probabilistic approach. In addition, we shall show that our method can be used to solve high-dimensional flow problems and the error estimate can be obtained in a straightforward way. In Section 5, we present numerical results to demonstrate the accuracy and efficiency of our method. We also investigate the convection enhanced diffusivity for several chaotic velocity fields, especially the three-dimensional cases. Concluding remarks are made in Section 6.

2. The definitions of the effective diffusivity

We first introduce the effective diffusivity for chaotic flows. The motion of a particle in a velocity field can be described by the following SDE,

$$\dot{X}(t) = v(X) + \sigma \xi(t), \quad X \in \mathbb{R}^d, \quad (2)$$

where $\sigma > 0$ is the molecular diffusion, X is the position of the particle, $v(X)$ is the Eulerian velocity field at position X , $\xi(t)$ is a Gaussian white noise with zero mean and correlation function $\langle \xi_i(t) \xi_j(t') \rangle = \delta_{ij} \delta(t - t')$. Here $\langle \cdot \rangle$ denotes the ensemble average over all randomness. To be consistent with the setting of main results in this paper, we assume the velocity $v(X)$ in (2) is time-independent. The interested reader is referred to [19, 29] and references therein for the results with time-dependent velocities.

There are two main frameworks to compute the effective diffusivity of the passive tracer models. We first discuss the Eulerian framework. Given any initial density $u_0(x)$, the particle

$X(t)$ of Eq.(2) has a density $u(x, t)$ that satisfies the Fokker-Planck equation,

$$u_t + \nabla \cdot (vu) = D_0 \Delta u, \quad u(x, 0) = u_0(x), \quad x \in \mathbb{R}^d, \quad (3)$$

where $D_0 = \sigma^2/2$ is the diffusion coefficient. When $v(x)$ is incompressible (i.e. $\nabla_x \cdot v(x) = 0$), deterministic and periodic in $O(1)$ scale, where we assume the period of $v(x)$ is 1 in space, the formula for the effective diffusivity matrix is [3, 26]

$$D^E = D_0 I - \langle v(x) \otimes \chi(x) \rangle_p, \quad (4)$$

where we have assumed that the fluid velocity $v(x)$ is smooth and the (vector) corrector field $\chi(x)$ satisfies the cell problem

$$-D_0 \Delta \chi + v(y) \cdot \nabla \chi = -v(y), \quad y \in \mathbb{T}^d, \quad (5)$$

and $\langle \cdot \rangle_p$ denotes spatial average over \mathbb{T}^d . Since $v(x)$ is incompressible, the solution $\chi(x)$ to the cell problem (5) is unique up to an additive constant by the Fredholm alternative. The correction to D_0 is positive definite in Eq.(4). By using L_2 -estimate of χ in Eq.(5), we can simply arrive at,

$$D^E \preceq \frac{1}{D_0}, \quad \text{as } D_0 \rightarrow 0. \quad (6)$$

More details of the derivation can be found in [4]. By multiplying χ to Eq.(5) and integrating in \mathbb{T}^d with consideration of periodicity of χ and v , we will get another formula for the effective diffusivity,

$$D^E = D_0 I + D_0 \langle \nabla \chi(x) \otimes \nabla \chi(x) \rangle_p. \quad (7)$$

We can see that $D^E \geq D_0$, this is called convection-enhanced diffusion. The residual diffusivity phenomenon that we studied in [29] is one case. While the upper bound of Eq.(6) is another case, which is called convection-enhanced diffusion with maximal enhancement [21].

In practice, the cell problem (5) can be solved using numerical methods, such as spectral methods. In [18], a small set of adaptive basis functions were constructed from fully resolved spectral solutions to reduce the computation cost. However, when D_0 becomes extremely small, the solutions of the advection-diffusion equation Eq.(5) develop sharp gradients and demand a large number of Fourier modes to resolve, which makes the Eulerian framework computationally expensive and unstable.

Alternatively, one can use the Lagrangian framework to compute the effective diffusivity tensor, which is defined by (equivalent to Eq.(4) via the homogenization theory)

$$D_{ij}^E = \lim_{t \rightarrow \infty} \frac{\langle (x_i(t) - x_i(0))(x_j(t) - x_j(0)) \rangle_r}{2t}, \quad 1 \leq i, j \leq d, \quad (8)$$

where $X(t) = (x_1(t), \dots, x_d(t))^T$ is the position of a particle tracer at time t and the average $\langle \cdot \rangle_r$ is taken over an ensemble of test particles. If the above limit exists, that means the transport of the particle is a standard diffusion process, at least on a long-time scale. If

the passive tracer model has a deterministic divergence-free and periodic velocity field, this is the typical situation, i.e., the spreading of the particle $\langle (x_i(t) - x_i(0))(x_j(t) - x_j(0)) \rangle_r$ grows linearly with respect to the time t . For example when the velocity field is given by the Taylor-Green velocity field [6, 27], the long-time and large-scale behavior of the passive tracer model is a diffusion process. However, there are also cases showing that the spreading of particles does not grow linearly with time but has a power law t^γ , where $\gamma > 1$ and $\gamma < 1$ correspond to super-diffusive and sub-diffusive behaviors, respectively [4, 19, 2].

We shall consider the Lagrangian approach in this paper. The Lagrangian framework has the advantages that it is easy to implement and does not directly suffer from a small molecular diffusion coefficient σ during the computation. However, we should point out that the major difficulty in solving Eq.(2) comes from the fact that the computational time should be long enough to approach the diffusion time scale. To address this challenge, we shall develop robust numerical integrators, which are structure-preserving and accurate for long-time integration. Moreover, we aim to develop the convergence analysis of the proposed numerical integrators in long-time integration. Finally, we shall investigate the relationship between several typical chaotic flows and the corresponding effective diffusivity.

3. Symplectic stochastic integrators

3.1. Derivation of numerical integrators

To demonstrate the main idea, we construct the new stochastic integrators for a two-dimensional passive tracer model with a separable Hamiltonian,

$$\begin{cases} dp = -f(q)dt + \sigma dW_{1,t}, & p(0) = p_0, \\ dq = g(p)dt + \sigma dW_{2,t}, & q(0) = q_0, \end{cases} \quad (9)$$

where $dW_{i,t}$ are independent Brownian motions and we have assumed that there exists a separable Hamiltonian function $H(p, q) = F(q) + G(p)$ such that $f(q) = H_q(p, q)$, $g(p) = H_p(p, q)$, and $H(p, q)$ is a periodic function on \mathbb{R}^2 with period 1. Furthermore, we assume that $H(p, q)$ is sufficiently smooth so the first order derivatives of $f(q)$ and $g(p)$ are bounded, which guarantee the existence and uniqueness of the solution (p, q) to the SDE (9).

In [29], we proposed a structure-preserving scheme based on an operator splitting idea to solve the SDE (9). Specifically, we split the SDE (9) into a deterministic subproblem (i.e., $dp = -f(q)dt$ and $dq = g(p)dt$) that is solved using a symplectic-preserving scheme and a random subproblem (i.e., $dp = \sigma dW_{1,t}$ and $dq = \sigma dW_{2,t}$) that is solved using the Euler-Maruyama scheme [23].

Now, we discuss how to discretize the SDE (9) using the Lie-Trotter splitting method. From time $t = t_n$ to time $t = t_{n+1}$, where $t_{n+1} = t_n + \Delta t$, $t_0 = 0$, assuming the solution $(p_n, q_n)^T \equiv (p(t_n), q(t_n))^T$ is given, we discretize the deterministic subproblem by

$$\begin{cases} p_* = p_n - \tau H_q(\alpha p_* + (1 - \alpha)p_n, (1 - \alpha)q_* + \alpha q_n), \\ q_* = q_n + \tau H_p(\alpha p_* + (1 - \alpha)p_n, (1 - \alpha)q_* + \alpha q_n), \end{cases} \quad (10)$$

where the parameters $\alpha \in [0, 1]$. Notice that $\alpha \in [0, 1]$ gives the same convergence rate. Then, we find that the exact solution of the random subproblem can be approximated by,

$$\begin{cases} p_{n+1} = p_* + \sigma \Delta_n W_1(\Delta t), \\ q_{n+1} = q_* + \sigma \Delta_n W_2(\Delta t), \end{cases} \quad (11)$$

with $\Delta_n W_i(\Delta t) = W_i(t_n + \Delta t) - W_i(t_n)$, $i = 1, 2$. In practice, each $\Delta_n W_i(\Delta t)$ is represented by an independent random variable of the form $\sqrt{\Delta t} \mathcal{N}(0, 1)$. In this paper, we choose $\alpha = 1$ in the scheme (10) and combine the two schemes (10)(11) together and obtain,

$$\begin{cases} p_{n+1} = p_n - f(q_n)\Delta t + \sigma\sqrt{\Delta t}\mathcal{N}(0, 1) \\ q_{n+1} = q_n + g(p_n - f(q_n)\Delta t)\Delta t + \sigma\sqrt{\Delta t}\mathcal{N}(0, 1). \end{cases} \quad (12)$$

We denote the stochastic process generated by (12) as $X_n = (p_n, q_n)$, which is the numerical approximation to the exact solution $X(n\Delta t)$ to the SDE (9).

Though there are several prior works on developing symplectic-preserving scheme for solving ODEs and PDEs (see [12, 13, 1] and references therein), the novelty of our paper is the rigorous theory in the numerical error analysis in computing the effective diffusivity. When the Hamiltonian system contains additive temporal noise, the noise itself is considered to be symplectic [22]. Since the symplectic scheme is a convergent symplectic transform and a composition of symplectic transform still preserves symplecticity. Thus, the scheme (12) is a symplectic-preserving scheme.

Remark 3.1. In general, the second-order Strang splitting [28] is more frequently adopted to solve ODEs and PDEs. The only difference between the Strang splitting method and the Lie-Trotter splitting method is that the first and last steps are modified by half of the time-step Δt . For the SDEs, however, the dominant source of error comes from the random subproblem (11). Thus, it is not necessary to implement the Strang splitting scheme.

3.2. The backward Kolmogorov equation and related results

For the convenience of the reader, we first give a brief review of the theoretical results for the scheme (12) obtained in [29] and references therein. One natural way to study the expectation of the paths for the SDE given by the Eq.(9) is to consider its associated backward Kolmogorov equation. Specifically, we associate the SDE with a partial differential operator \mathcal{L} , which is called the generator of the SDE, also known as the flow operator.

$$u_t = \mathcal{L}u, \quad u(x, 0) = u_0(x), \quad (13)$$

where the operator \mathcal{L} is given by

$$\mathcal{L} = -f\partial_q + g\partial_p + \frac{1}{2}\sigma^2\partial_p^2 + \frac{1}{2}\sigma^2\partial_q^2. \quad (14)$$

A probabilistic interpretation of Eq.(13) is that given initial density $u_0(x)$ and a smooth function ϕ in \mathbb{R}^2 , the solution to the Eq.(13), $u(x, t)$ satisfies $u(x, t) = \mathbb{E}(\phi(X_t)|X_0 = x)$, where $X_t = (p(t), q(t))$ is the solution to the Eq.(9).

Similar to (13), we can study the flow generated by symplectic splitting scheme. Recall that the Hamiltonian of the Eq.(9) is separable. We define $\mathcal{L}_1 = -f\partial_p$, $\mathcal{L}_2 = g\partial_q$, and $\mathcal{L}_3 = \frac{\sigma^2}{2}(\partial_{pp} + \partial_{qq})$. Starting from $u(\cdot, 0)$, we compute

$$\begin{cases} \partial_t u^1 &= \mathcal{L}_1 u^1, & u^1(\cdot, 0) = u(\cdot, 0), \\ \partial_t u^2 &= \mathcal{L}_2 u^2, & u^2(\cdot, 0) = u^1(\cdot, \Delta t), \\ \partial_t u^3 &= \mathcal{L}_3 u^3, & u^3(\cdot, 0) = u^2(\cdot, \Delta t), \end{cases} \quad (15)$$

and obtain $u(\cdot, \Delta t) \approx u^3(\cdot, \Delta t)$. We can repeat this process to compute the solution at other time steps $u(\cdot, n\Delta t)$, $n = 2, 3, \dots$

To analyze the error between the flow operator in Eq.(13) and the operator associated with the symplectic splitting (15), we shall resort to the Baker-Campbell-Hausdorff (BCH) formula, which is widely used in non-commutative algebra [11]. For example, in the martix theory,

$$\exp(At)\exp(Bt) = \exp\left(t(A+B) + t^2\frac{[A,B]}{2} + \frac{t^3}{12}\left([A,[A,B]] + [B,[B,A]]\right) + \dots\right), \quad (16)$$

where t is a scalar, A, B are two square matrices with the same size, $[,]$ is the Lie-Bracket, and the remaining terms on the right hand side are all nested Lie-brackets.

In our analysis, we replace the matrices in (16) by PDE operators and the BCH formula yields some insights into the particular structure of splitting errors. Let $I_{\Delta t}$ denote the flow operator associated with the symplectic splitting (15), i.e.,

$$u(\cdot, \Delta t) \approx I_{\Delta t}u(\cdot, 0) = \exp(\Delta t\mathcal{L}_3)\exp(\Delta t\mathcal{L}_2)\exp(\Delta t\mathcal{L}_1)u(\cdot, 0). \quad (17)$$

Recall that the exact solution to the Eq.(13) can be represented as

$$u(\cdot, \Delta t) = \exp(\Delta t\mathcal{L})u(\cdot, 0) = \exp(\Delta t(\mathcal{L}_1 + \mathcal{L}_2 + \mathcal{L}_3))u(\cdot, 0). \quad (18)$$

Therefore, we can apply the BCH formula to analyze the error between the original flow and the approximated flow. Moreover, we find that to compute the k -th order modified equation associated with the Eq.(9) is equivalent to compute the terms of BCH formula up to order $(\Delta t)^k$. To show that the solution generated by (12) follows a perturbed Hamiltonian system (with divergence free velocity and additive noise) at any order p , we only need to consider the $(p+1)$ -nested Lie bracket consists of $\{-f\partial_q, g\partial_p, \partial_{pp} + \partial_{qq}\}$ and we can easily see that they will not generate non-divergence free field.

In [29], we proved that for the SDE (9) with a time-dependent and separable Hamiltonian $H(p, q, t) = F(p, t) + G(q, t)$, the numerical solution obtained using the symplectic-preserving scheme (12) follows an asymptotic Hamiltonian $H^{\Delta t}(p, q, t)$, which is a first-order approximation to $H(p, q, t)$. Equivalently, the solution to the first-order modified equation (density function) (15) is divergence-free and the invariant measure on torus (defined by $\mathbb{R}^d/\mathbb{Z}^d$, when period is 1) remains uniform, which is also known as the Haar measure. While the numerical solution obtained using the Euler-Maruyama scheme does not have these properties.

Moreover, given any explicit splitting scheme for deterministic systems, by adding additive noise we shall have similar form of flow propagation. And we shall see in later proof that, such operator formulation is very effective in analyzing the order of convergence and volume-preserving property.

4. Convergence analysis

We shall prove the convergence rate of our symplectic stochastic integrators in computing effective diffusivity based on a probabilistic approach, which allows us to get rid of the exponential growth factor in our error estimate.

4.1. Convergence to an invariant measure

The numerical method to compute effective diffusivity of a passive tracer model is closely related to study the limit of a sequence generated by the stochastic integrators. Therefore, we can apply the results from ergodic theory to study the convergence of the solution. The following result is fundamental for the proof of our convergence analysis.

Proposition 4.1. *On the torus space $\tilde{Y} = \mathbb{R}^d/\mathbb{Z}^d$, let $I_{\Delta t}^*$ denote the transform of the density function during Δt using the numerical scheme (12). Let $I_{\Delta t}$ denote the adjoint operator (i.e., the flow operator) of $I_{\Delta t}^*$ in space of $\mathcal{B}(\tilde{Y})$, which is the set of bounded measurable functions on \tilde{Y} . Then $I_{\Delta t}$ is a compact operator from $\mathcal{B}(\tilde{Y})$ to itself. And there exists one and only one invariant probability measure on (\tilde{Y}, Σ) , denoted as π , satisfying,*

$$\sup_{x \in \tilde{Y}} \left| I_{\Delta t}^n \phi(x) - \int \phi(x) \pi(dx) \right| \leq K \|\phi\|_{L^\infty} e^{-\rho n}, \quad \forall \phi \in \mathcal{B}(\tilde{Y}), \quad (19)$$

where $\rho > 0$, $K > 0$ are independent of $\phi(x)$.

Proof. We shall verify that the transition kernel associated with the numerical scheme (12) satisfies the assumptions required by the Theorem 3.3.1 (see the page 199 in [3]). First in the \mathbb{R}^n space, the integration process associated with the numerical scheme (12) can be expressed as a Markov process with the transition kernel,

$$K_{\Delta t}((p, q), (P, Q)) = \frac{1}{2\pi\sigma^2\Delta t} \exp\left(-\frac{\left(P - p + f(q)\Delta t\right)^2 + \left(Q - q - g(p - f(q)\Delta t)\Delta t\right)^2}{2\sigma^2\Delta t}\right), \quad (20)$$

where (p, q) is the current solution and (P, Q) is the solution obtained by applying the numerical integrator (12) on (p, q) with time step Δt .

Then using the periodicity of $f(x)$ and $g(x)$, we extend (20) directly to the torus space \tilde{Y} as

$$\tilde{K}_{\Delta t}((p, q), (P, Q)) = \sum_{i, j \in \mathbb{Z}} \frac{1}{2\pi\sigma^2\Delta t} \exp\left(-\frac{\left(P + i - p + f(q)\Delta t\right)^2 + \left(Q + j - q - g(p - f(q)\Delta t)\Delta t\right)^2}{2\sigma^2\Delta t}\right). \quad (21)$$

One can see that if $0 < \Delta t \ll 1$, then \tilde{K} is smooth and is essentially bounded above zero, i.e., $\text{essn } \tilde{K} > 0$, $\forall ((p, q), (P, Q)) \in \tilde{Y} \times \tilde{Y}$. Thus, the operator $I_{\Delta t}$ is compact since it is an integral operator with a smooth kernel. Then applying the Theorem 3.3.1 in [3], we prove the assertion of the Proposition 4.1. \square

Now, we state a corollary that is a simple conclusion of exponential decay property proved in Proposition 4.1. It will be useful in the proof of the main results of this paper.

Corollary 4.2. *Given that the assumptions in Proposition 4.1 are satisfied and $\phi \in \mathcal{B}(\tilde{Y})$, we have*

$$\lim_{n \rightarrow \infty} \frac{1}{n} \sum_{i=1}^n E\phi(X_i) = \int_{\tilde{Y}} \phi \pi(dx). \quad (22)$$

Before we close this subsection, we prove a convergence result for the inverse of operator sequences, which will be useful in our analysis.

Proposition 4.3. *Let X, Y denote two Banach spaces. Assume T_n, T are bounded linear operators from X to Y , satisfying $\lim_{n \rightarrow \infty} \|T_n - T\|_{\mathcal{B}(X, Y)} = 0$, and $T^{-1} \in \mathcal{B}(Y, X)$. Then, given $f \in Y$ with 'enough' invertibility (i.e. $T^{-1}f$ and $T_n^{-1}f$, $n = 1, 2, \dots$ exist), we have*

$$\lim_{n \rightarrow \infty} \|(T_n^{-1} - T^{-1})f\| = 0 \quad (23)$$

Proof. After some simple calculations, we get

$$\begin{aligned} T_n^{-1} - T^{-1} &= T^{-1}(T - T_n)T_n^{-1} \\ &= T^{-1}(T - T_n)T^{-1} + T^{-1}(T - T_n)(T_n^{-1} - T^{-1}). \end{aligned} \quad (24)$$

Now applying $T_n^{-1} - T^{-1}$ on f , we get

$$\begin{aligned} \|(T_n^{-1} - T^{-1})f\| &\leq \|T^{-1}\|^2 \cdot \|T - T_n\| \cdot \|f\| \\ &\quad + \|T^{-1}\| \cdot \|T - T_n\| \cdot \|(T_n^{-1} - T^{-1})f\| \end{aligned} \quad (25)$$

Since $\lim_{n \rightarrow \infty} \|T_n - T\| = 0$, we assume for $n \geq N_0$, $\|T_n - T\| \cdot \|T^{-1}\| < \frac{1}{2}$, then,

$$\|(T_n^{-1} - T^{-1})f\| \leq 2\|T^{-1}\|^2 \cdot \|T - T_n\| \cdot \|f\|, \quad \forall n \geq N_0, \quad (26)$$

Eq.(23) follows if we take the limit as $n \rightarrow \infty$ on both sides. \square

4.2. A discrete-type cell problem

In the Eulerian framework, the periodic solution of the cell problem (5) and the corresponding formula for the effective diffusivity (4) play a key role in studying the behaviors of the chaotic and stochastic flows. In the Lagrangian framework, we shall define a discrete analogue of the cell problem that enables us to compute the effective diffusivity. Let $X_n = (p_n, q_n)$ denote the state generated by our scheme (12), i.e.,

$$\begin{cases} p_n = p_{n-1} - f(q_{n-1})\Delta t + \sigma N_{n-1}^p \\ q_n = q_{n-1} + g(p_{n-1} - g(q_{n-1})\Delta t)\Delta t + \sigma N_{n-1}^q, \end{cases} \quad (27)$$

where $N_{n-1}^p, N_{n-1}^q \sim \sqrt{\Delta t} \mathcal{N}(0, 1)$ are i.i.d. normal random variables.

We will show that the solution obtained using the scheme (27) has a bounded expectation. Taking expectation of the first equation of (27) on both sides, we obtain

$$Ep_n = Ep_{n-1} - \Delta t Ef(q_{n-1}) = Ep_0 - \Delta t \sum_{k=0}^{n-1} Ef(q_k). \quad (28)$$

Applying the Proposition 4.1 and using the fact that f is a periodic function, we know that $|Ef(q_k)| \leq e^{-\rho n} \|f\|_\infty$. Hence

$$Ep_n \leq |Ep_0| + C_1 \|f\|_\infty, \quad (29)$$

where C_1 does not depend on n . Using the same approach, we know that Eq_n is also bounded. Now we are in the position to define the discrete-type cell problem. We first define

$$\hat{f}(x) = -\Delta t \sum_{n=0}^{\infty} E[f(X_n)|X_0 = x], \quad x \in \tilde{Y}. \quad (30)$$

Then, we shall show that $\hat{f}(x)$ satisfies the following properties.

Lemma 4.4. *Assume that f is a periodic function with zero mean on \tilde{Y} . Then, $\hat{f}(x)$ is the unique solution in $\mathcal{B}_0(\tilde{Y})$ such that,*

$$\hat{f}(X_0) + \Delta t f(X_0) = E[\hat{f}(X_1)|X_0]. \quad (31)$$

Moreover, \hat{f} is smooth.

Proof. Throughout the proof, we shall use the fact that if x, y are random processes and y is measurable under a filtration \mathcal{F} , then with appropriate integrability assumption,

$$E[xy] = E\left[E[xy|\mathcal{F}]\right] = E\left[E[x|\mathcal{F}]y\right]. \quad (32)$$

Some simple calculations will give that

$$\begin{aligned} \hat{f}(X_0) + \Delta t f(X_0) &= \Delta t E\left[\sum_{m=0}^{\infty} -f(X_m)|X_0\right] + \Delta t f(X_0) = -\Delta t E\left[\sum_{m=1}^{\infty} f(X_m)|X_0\right] \\ &= -\Delta t E\left[E\left[\sum_{m=1}^{\infty} f(X_m)|X_1\right]|X_0\right] = E[\hat{f}(X_1)|X_0]. \end{aligned} \quad (33)$$

Recall the definition of the operator (17), Eq.(33) implies that

$$(I_{\Delta t} - I_d)\hat{f} = I_{\Delta t}\hat{f} - \hat{f} = \Delta t f, \quad (34)$$

where I_d is the identity operator. Moreover, since f is smooth and the mapping of the operator $I_{\Delta t}$ on bounded functions will generate smooth functions, so \hat{f} is smooth.

According to Proposition 4.1, the invariant measure of $I_{\Delta t}^*$ is unique, i.e. $\dim \mathcal{N}(I_{\Delta t}^* - I_d) = 1$. By the Fredholm alternative, we arrive at the conclusion that the solution \hat{f} to Eq.(34) is unique in $\mathcal{B}(\tilde{Y})$ up to a constant and it smoothly depends on f , given the assumption that $\int_{\tilde{Y}} f = 0$. \square

When the flow is time-independent, we obtain

$$E[\hat{f}(X_{n+1})|X_n] - \hat{f}(X_n) = \Delta t f(X_n), \quad a.s. \quad \forall n \in \mathbb{N}. \quad (35)$$

Remark 4.1. For the second component of the solution, i.e., q_n , we can define the discrete cell problem in the same manner. Specifically, we define

$$\hat{g}(x) = \Delta t \sum_{n=0}^{\infty} E[g(X'_n)|X_0 = x], \quad x \in \tilde{Y}, \quad (36)$$

where $X'_n = X_n - \Delta t f(X_n)$. There is no substantial difficulties in carrying out the analysis for $\hat{g}(x)$. Because under the assumption that the drift terms f and g in (9) are smooth enough, the leading order term of $g(X'_n)$ is $g(\tilde{X}_n)$ and other terms are small perturbations.

The Proposition 4.1 and the Lemma 4.4 are very general results. In the remaining part of this paper, we only need the result that \hat{f} is unique in an Hölder space $\mathbb{C}_0^{p,\alpha}(\tilde{Y}) \subsetneq \mathcal{B}(\tilde{Y})$. To be precise, given a smooth drift function f , \hat{f} shall be in $\mathbb{C}_0^{p,\alpha}(\tilde{Y})$, where $p \geq 6, 0 < \alpha < 1$ and the subscript index 0 indicates that it is a subspace with zero-mean functions. Since $I_{\Delta t}$ is an integral operator with a smooth kernel, to prove it is a compact operator from $\mathbb{C}_0^{p,\alpha}(\tilde{Y})$ to itself, we only need to verify that it is a bounded linear operator and then use compact embedding theorem. The uniqueness can also be approached by maximum principle. However, we do not want to complicate the presentation by pursuing this avenue.

4.3. Convergence estimate of the discrete-type cell problem

After defining the discrete-type cell problem (e.g., Eq.(34)) and proving the existence and uniqueness of the solution \hat{f} , we shall prove that \hat{f} converges to the solution of a continuous cell problem in certain subspace, e.g., $\mathbb{C}_0^{6,\alpha}(\tilde{Y})$. To start with, we define the following continuous cell problem

$$\mathcal{L}\chi_1 = f, \quad (37)$$

where the operator \mathcal{L} is defined in (14). Given f is smooth enough and periodic, the Eq.(37) admits a solution χ_1 in $\mathbb{C}^{6,\alpha}(\tilde{Y})$. This is a standard result of the elliptic PDEs in Hölder space (see, e.g., the Theorem 6.5.3 in [15]). From the Eq.(37), some calculations will give

$$\exp(\Delta t \mathcal{L})\chi_1 - \chi_1 = f\Delta t + \mathcal{O}(\Delta t^2) := \Delta t \bar{f}, \quad (38)$$

where $\bar{f} = f + \mathcal{O}(\Delta t)$. Combining Eqns.(34) and (38), we obtain

$$(\exp(\Delta t \mathcal{L}) - I_d)(\chi_1 - \hat{f}) = (I_{\Delta t} - \exp(\Delta t \mathcal{L}))\hat{f} + \Delta t(\bar{f} - f). \quad (39)$$

Eq.(39) shows the connection between χ_1 and \hat{f} . We rewrite it as

$$\tilde{L}_1(\chi_1 - \hat{f}) = \tilde{L}_2\hat{f} + (\bar{f} - f), \quad (40)$$

where

$$\tilde{L}_1 := \frac{(\exp(\Delta t \mathcal{L}) - I_d)}{\Delta t}, \quad \tilde{L}_2 := \frac{I_{\Delta t} - \exp(\Delta t \mathcal{L})}{\Delta t}. \quad (41)$$

To estimate the convergence rate between \hat{f} and χ_1 , we need to study the operators \tilde{L}_1 and \tilde{L}_2 in the Eq.(40).

We first show that the inverse of \tilde{L}_1 is a continuous bijection between subspace of invertible operator and subspace of its inversion. We can easily verify that in the space of bounded linear operators from $\mathbb{C}^{6,\alpha}(\tilde{Y})$ to $\mathbb{C}^{4,\alpha}(\tilde{Y})$ and we have the strong convergence in the operator norm,

$$\tilde{L}_1 \rightarrow \mathcal{L} \quad \text{as } \Delta t \rightarrow 0. \quad (42)$$

Applying the convergence result of the Proposition 4.3, for the inverse of the operator \tilde{L}_1 , we get

$$\lim_{\Delta t \rightarrow 0} \hat{f} = \lim_{\Delta t \rightarrow 0} \tilde{L}_1^{-1} f = \mathcal{L}^{-1} f = \chi_1. \quad (43)$$

Then, we study the operator \tilde{L}_2 . Using the BCH formula(16), we obtain

$$\begin{aligned} \tilde{L}_2 \hat{f} &\rightarrow \frac{\exp\left(\frac{\Delta t^2}{2}([L_3, L_2] + [L_2, L_1] + [L_3, L_1]) + \mathcal{O}(\Delta t^3)\right) - I_d}{\Delta t} \cdot \exp(\Delta t \mathcal{L}) \\ &\rightarrow \frac{\Delta t}{2}([L_3, L_2] + [L_2, L_1] + [L_3, L_1]) + \mathcal{O}(\Delta t^2). \end{aligned} \quad (44)$$

Combining Eqns. (40)(43) and (44), we know that if Δt is small enough (does not depend on the total computational time T , but may depend on estimate of f , g and σ), the following convergence estimate holds

$$\chi_1 - \hat{f} = \mathcal{O}(\Delta t). \quad (45)$$

Finally, we summarize the above convergence estimate result into a Lemma as follows.

Lemma 4.5. *When $\Delta t \rightarrow 0$, the solution \hat{f} to the discrete-type cell problem converges to the solution to cell problem χ_1 in $\mathbb{C}_0^{p,\alpha}$, at the rate of $\mathcal{O}(\Delta t)$, where $p \geq 6$ and $0 < \alpha < 1$.*

4.4. Convergence estimate for the effective diffusivity

We shall show the main estimates in this section. We first prove that the second-order moment of the solution obtained by using our numerical scheme has an (at most) linear growth rate. Secondly, we provide the convergence analysis of our method in computing the effective diffusivity.

Theorem 4.6. *Let $X_n^{\Delta t} = (p_n, q_n)$ denote the solution obtained by using our numerical scheme with time-step Δt . With general assumptions mention before, the second moment of the solution $X_n^{\Delta t}$ (a discrete Markov process) is at most linear growth, i.e.,*

$$\max_n \left\{ \mathbb{E} \frac{\|X_n^{\Delta t}\|^2}{n} \right\} \text{ is bounded.} \quad (46)$$

Proof. We first estimate the second-order moment of the first component of $X_n^{\Delta t} = (p_n, q_n)$, since the other one can be estimated in the same manner. Simple calculations show that

$$\begin{aligned} E[p_n^2 | (p_{n-1}, q_{n-1})] &= E(p_{n-1} - f(q_{n-1})\Delta t + \sigma N_{i-1}^p)^2 \\ &= E p_{n-1}^2 + \Delta t (\sigma^2 - 2E[p_{n-1} f(q_{n-1})]) + \Delta t^2 E f^2(q_{n-1}). \end{aligned} \quad (47)$$

We should point out that the term $E[p_{n-1}f(q_{n-1})]$ corresponds to the convection enhanced level of the diffusivity. Our goal is to prove that the term $E[p_{n-1}f(q_{n-1})]$ is bounded over n , though it may depend on f , g and σ . We now directly compute the contribution of the term $E[p_{n-1}f(q_{n-1})]$ to the effective diffusivity with the help of Eq.(35), i.e.,

$$\Delta t \sum_{i=0}^{n-1} E[p_i f(q_i)] = \sum_{i=0}^{n-1} E[p_i (E[\hat{f}(X_{i+1})|X_i] - \hat{f}(X_i))]. \quad (48)$$

Let \mathcal{F}_i denote the filtration generated by the solution process until X_i . Notice that $p_i \in \mathcal{F}_i$, for the Eq.(48), we have

$$\begin{aligned} RHS &= \sum_{i=0}^{n-1} E[p_i (\hat{f}(X_{i+1}) - \hat{f}(X_i))] \\ &= \sum_{i=1}^n E[\hat{f}(X_i)(p_{i-1} - p_i)] - \hat{f}(X_0)p_0 + E[\hat{f}(X_n)p_n] \\ &= \sum_{i=1}^n E[\hat{f}(X_i)(f(p_{i-1})\Delta t - \sigma N_{i-1}^p)] - \hat{f}(X_0)p_0 + E[\hat{f}(X_n)p_n]. \end{aligned} \quad (49)$$

Hence,

$$\begin{aligned} \frac{1}{n}E[p_n^2|(p_0, q_0)] &= \frac{1}{n}p_0^2 + \Delta t\sigma^2 - 2\Delta t\frac{1}{n}\sum_{i=0}^{n-1} E[p_i f(q_i)] + (\Delta t)^2\frac{1}{n}\sum_{i=0}^{n-1} E f^2(q_i) \\ &= \frac{1}{n}p_0^2 + \Delta t\sigma^2 + (\Delta t)^2\frac{1}{n}\sum_{i=0}^{n-1} E f^2(q_i) - \frac{2}{n}\sum_{i=1}^n E[\hat{f}(X_i)(f(q_{i-1})\Delta t - \sigma N_{i-1}^p)] \\ &\quad - \frac{2}{n}(\hat{f}(X_0)p_0 - E[\hat{f}(X_n)p_n]). \end{aligned} \quad (50)$$

Recall the fact that $X_n = (p_n, q_n)$ converges to the uniform measure in distribution. So given any continuous periodic function f^* , the Corollary 4.2 implies

$$\lim_{n \rightarrow \infty} E f^*(X_n) = \int_{\tilde{Y}} f^*(x) dx. \quad (51)$$

Furthermore, we have the estimate

$$\limsup_{n \rightarrow \infty} \frac{1}{n} \sum_{i=0}^n f^*(X_n) < \infty. \quad (52)$$

Applying the Cauchy-Schwarz inequality for the term $\frac{2}{n} \sum_{i=1}^n E[\hat{f}(X_i)(f(q_{i-1})\Delta t - \sigma N_{i-1}^p)]$ in (50) and replacing f^* by f^2 and \hat{f}^2 in (52), we can prove that $\frac{1}{n}E[p_n^2|(p_0, q_0)]$ is bounded. Repeat the same trick, we know that $\frac{1}{n}E[q_n^2|(p_0, q_0)]$ is also bounded. Thus, the assertion in (46) is proved. \square

In our numerical scheme (12), we first fix the time-step Δt and use the scheme (12) to compute the effective diffusivity until the result converges to a constant, which may depend on Δt . Then, we shall prove that the limit of the constant converges to the exact effective diffusivity of the original passive tracer model as Δt approaches zero. Namely, we aim to prove that our numerical scheme (12) is robust in computing the effective diffusivity.

Theorem 4.7. *Let p_n , $n = 0, 1, \dots$ be the numerical solution of the first component of the scheme (12) and Δt denote the time-step. We have the convergence estimate of the effective diffusivity as*

$$\lim_{n \rightarrow \infty} \frac{E p_n^2}{n \Delta t} = \sigma^2 - 2 \int_{\mathbb{T}^2} \chi_1 f + \mathcal{O}(\Delta t), \quad (53)$$

where the constant in $\mathcal{O}(\Delta t)$ only depends on f .

Proof. We divide both sides of the Eq.(50) by Δt and obtain

$$\begin{aligned} \frac{1}{n \Delta t} E[p_n^2 | (p_0, q_0)] &= \frac{1}{n \Delta t} p_0^2 + \sigma^2 + \frac{\Delta t}{n} \sum_{i=0}^{n-1} E f^2(q_i) \\ &\quad - \frac{2}{n \Delta t} \sum_{i=1}^n E[\hat{f}(X_i)(f(q_{i-1})\Delta t - \sigma N_{i-1}^p)] \\ &\quad - \frac{2}{n \Delta t} (\hat{f}(X_0)p_0 - E[\hat{f}(X_n)p_n]) \end{aligned} \quad (54)$$

First, we notice that for a fixed Δt , the terms $\frac{1}{n \Delta t} p_0^2$ and $\frac{2}{n \Delta t} \hat{f}(X_0)p_0$ converge to zero as $n \rightarrow \infty$, where we have used the fact $\hat{f}(X_0)$ is bounded. Then, for a fixed Δt , we have

$$\lim_{n \rightarrow \infty} \frac{2}{n \Delta t} |E[\hat{f}(X_n)p_n]| \leq \lim_{n \rightarrow \infty} \frac{2}{\sqrt{n} \Delta t} \|\hat{f}\|_\infty E\left|\frac{p_n}{\sqrt{n}}\right| \leq \lim_{n \rightarrow \infty} \frac{1}{\sqrt{n} \Delta t} \|\hat{f}\|_\infty E\left[\frac{p_n^2}{n} + 1\right] = 0, \quad (55)$$

where the term $E\left[\frac{p_n^2}{n}\right]$ is bounded due to the Theorem 4.6 and $\|\hat{f}\|_\infty \rightarrow \|\chi_1\|_\infty$ due to the Lemma 4.5.

Therefore, we only need to focus on the estimate of terms in the second line of (54). Notice that $\hat{f} \in \mathbb{C}^{6,\alpha}$, we compute the Ito-Taylor series approximation of $\hat{f}(X_i)$,

$$\begin{aligned} \hat{f}(X_i) &= \hat{f}(X_{i-1}) + \hat{f}_p(X_{i-1})(-f(q_{i-1})\Delta t + \sigma N_{i-1}^p) + \hat{f}_q(X_{i-1})(g(p_{i-1})\Delta t + \sigma N_{i-1}^q) \\ &\quad + \frac{1}{2}(\hat{f}_{pp}(X_{i-1}) + \hat{f}_{qq}(X_{i-1}))\sigma^2 \Delta t + \mathcal{O}(\Delta t^2). \end{aligned} \quad (56)$$

Since $\hat{f} \rightarrow \chi_1$ in $\mathbb{C}_0^{6,\alpha}$, the truncated term $\mathcal{O}(\Delta t^2)$ in Eq.(56) is uniformly bounded when Δt is small enough. Substituting the Taylor expansion of $\hat{f}(X_i)$ into the target term of our estimate, we get

$$\begin{aligned} E[\hat{f}(X_i)(f(q_{i-1})\Delta t - \sigma N_{i-1}^p)] &= E\left[\left(f(q_{i-1})\Delta t - \sigma N_{i-1}^p\right) \right. \\ &\quad \left. \left(\hat{f}(X_{i-1}) + \hat{f}_p(X_{i-1})(-f(q_{i-1})\Delta t + \sigma N_{i-1}^p) \right. \right. \\ &\quad \left. \left. + \hat{f}_q(X_{i-1})(g(p_{i-1})\Delta t + \sigma N_{i-1}^q) + \frac{1}{2}(\hat{f}_{pp}(X_{i-1}) + \hat{f}_{qq}(X_{i-1}))\sigma^2 \Delta t + \mathcal{O}(\Delta t^2)\right)\right]. \end{aligned} \quad (57)$$

Combining the terms with the same order of Δt , we obtain

$$E[\hat{f}(X_i)(f(q_{i-1})\Delta t - \sigma N_{i-1}^p)] = \Delta t E[\hat{f}(X_{i-1})f(q_{i-1}) - \sigma^2 \hat{f}_p(X_{i-1})] + \mathcal{O}(\Delta t^2), \quad (58)$$

where we have used the facts and $X_{i-1} \perp (N_{i-1}^p, N_{i-1}^q)$, $N_{i-1}^p \perp N_{i-1}^q$ and $E(N_{i-1}^p)^2 = \Delta t$. Finally, by using the Corollary 4.2 and noticing the invariant measure is the uniform measure, we obtain from Eq.(54) that

$$\lim_{n \rightarrow \infty} \frac{1}{n\Delta t} E[p_n^2 | (p_0, q_0)] = \sigma^2 - 2 \int (\hat{f}f - \sigma^2 \hat{f}_p) + \mathcal{O}(\Delta t). \quad (59)$$

Thus, the Eq.(53) is proved as a result of Lemma 4.5 and $\int \hat{f}_p = 0$. \square

4.5. Generalizations to high-dimensional cases

To show the essential idea of our probabilistic approach, we have carried out our convergence analysis based on a two-dimensional model problem (9). In fact, the extension of our approach to higher-dimensional problems is straightforward. Now we consider a high-dimensional problem as follow,

$$dX_t = v(X_t)dt + \Sigma dW_t, \quad (60)$$

where $X = (X^1, X^2, \dots, X^d)^T \in R^d$ is the position of the particle, $v = (v^1, v^2, \dots, v^d)^T \in R^d$ is the Eulerian velocity field at position X , Σ is a $d \times d$ constant non-singular matrix, and dW_t is a d -dimension Brownian motion vector. In particular, we assume the v^i does not depend on X^i , $i = 1, \dots, d$. Thus, the incompressible condition for $v(X)$ (i.e. $\nabla_X \cdot v(X) = 0$) is easily guaranteed.

For a deterministic and divergence-free dynamic system, Feng et. al. proposed a volume-preserving method [8], which splits an n -dimensional problem into $n - 1$ subproblems with each of them being volume-preserving. We shall modify Feng's method (first order case) by including the randomness as the last subproblem to take into account the additive noise, i.e.,

$$\begin{cases} X^{1*} = X_0^1 + \Delta t v^1(X_0^1, X_0^2, X_0^3, \dots, X^{d-1}, X_0^d), \\ X^{2*} = X_0^2 + \Delta t v^2(X_0^{1*}, X_0^2, X_0^3, \dots, X^{d-1}, X_0^d), \\ \dots, \\ X^{d*} = X_0^d + \Delta t v^d(X_0^{1*}, X_0^{2*}, X_0^{3*}, \dots, X^{(d-1)*}, X_0^d), \\ X_1 = X^* + \Sigma(W_1 - W_0), \end{cases} \quad (61)$$

where $W_1 - W_0$ is represented by a d -dimensional independent random vector with each component of the form $\sqrt{\Delta t} \mathcal{N}(0, 1)$.

The techniques of the convergence analysis for two-dimensional problem can be applied to high-dimensional problems without much difficulty. For the high-dimensional problem (60), the smoothness and strict positivity of the transition kernel in the discrete process can be guaranteed if one assumes that the covariance matrix Σ is non-singular and the scheme (61) is explicit. According to our assumption for the velocity field, the scheme (61) is

volume-preserving. Thus, the solution to the first-order modified equation is divergence-free and the invariant measure on torus (defined by $\mathbb{R}^d/\mathbb{Z}^d$, when period is 1) remains uniform. Finally, the convergence of cell problem can be achieved by using the BCH formula (16) with $d + 1$ stage splitting. Therefore, our numerical methods are robust in computing effective diffusivity for high-dimensional problems, which will be demonstrated through the three-dimensional chaotic flow problems in the Section 5.

5. Numerical Examples

The aim of this section is two-fold. First, we shall design challenging numerical examples to verify the convergence analysis proposed in this paper, especially the Theorem 4.7. Secondly, we shall investigate the existence of residual diffusivity for several chaotic velocity fields. Without loss of generality, we compute the quantity $\frac{E[p(T)^2]}{2T}$, which is used to approximate D_{11}^E in the effective diffusivity matrix (4).

5.1. Verification of the convergence rate

We first consider a passive tracer model where the velocity field is given by a chaotic cellular flow with oscillating vortices. Specifically, the flow is generated by a Hamiltonian defined as

$$H(p, q) = \frac{1}{2\pi} \exp(\sin(2\pi p)) - \frac{1}{4\pi} \exp(\cos(4\pi q + 1)). \quad (62)$$

The motion of a particle moving in this chaotic cellular flow is described by the SDE,

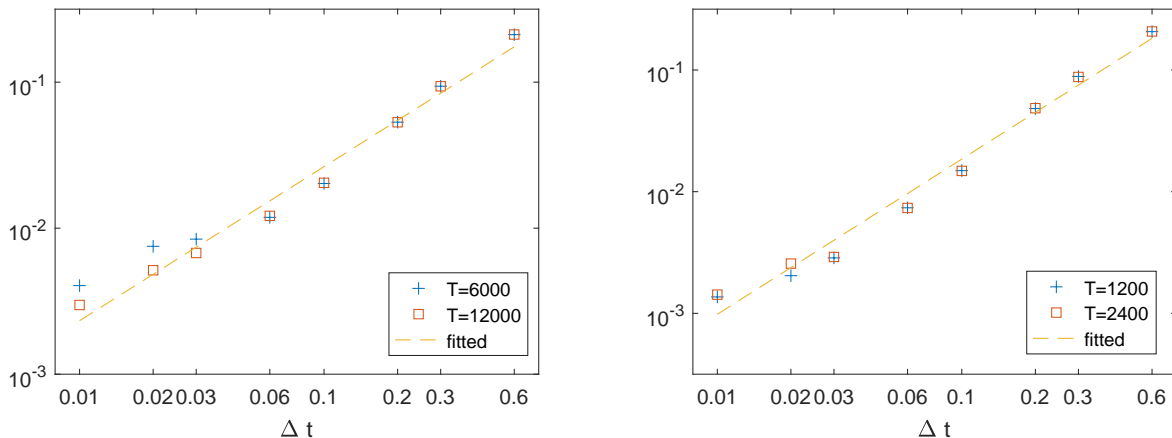
$$\begin{cases} dp = \sin(4\pi q + 1) \exp(\cos(4\pi q + 1))dt + \sigma dW_1, \\ dq = \cos(2\pi p) \exp(\sin(2\pi p))dt + \sigma dW_2, \end{cases} \quad (63)$$

where $\sigma = \sqrt{2 \times 0.01}$, dW_i are independent Brownian motions, and the initial data (p_0, q_0) follows uniform distributions in $[-0.5, 0.5]^2$.

In our numerical experiments, we use Monte Carlo samples to discretize the Brownian motions dW_1 and dW_2 . The sample number is denoted by N_{mc} . We choose $\Delta t_{ref} = 0.001$ and $N_{mc} = 640,000$ to solve the SDE (63) and compute the reference solution, i.e., the ‘‘exact’’ effective diffusivity, where the final computational time is $T = 12000$ so that the calculated effective diffusivity converges to a constant. It takes about 20 hours to compute the reference solution on a 64-core server (Gridpoint System at HKU). The reference solution for the effective diffusivity is $D_{11} = 0.12629$.

In Fig.1a, we plot the convergence results of the effective diffusivity using our method (i.e., $\frac{E[p(T)^2]}{2T}$) with respect to different time-step Δt at $T = 6000$ and $T = 12000$. In addition, we show a fitted straight line with the slope 1.04, i.e., the convergence rate is about $(\Delta t)^{1.04}$. Meanwhile, by comparing two sets of data in the Figs.1a and 1b, corresponding to the numerical effective diffusivity obtained at different computational times, we can see that error does not grow with respect to time, which justifies the statement in Theorem 4.7.

To further study the adaptability and robustness of our numerical method in solving high-dimensional problems, we consider a 3D Kolmogorov-type flow. Let $(p, q, r) \in R^3$ denote



(a) 2D chaotic cellular flow, fitted slope ≈ 1.04 (b) 3D Kolmogorov-type flow, fitted slope ≈ 1.27

Figure 1: Error of D_{11}^E in different computational times and flows with different time-steps.

the position of a particle in the 3D Cartesian coordinate system. The motion of a particle moving in the 3D Kolmogorov-type flow is described by the following SDE,

$$\begin{cases} dp = \cos(4\pi r + 1) \exp(\sin(4\pi r + 1))dt + \sigma dW_1, \\ dq = \cos(6\pi p + 2) \exp(\sin(6\pi p + 2))dt + \sigma dW_2, \\ dr = \cos(2\pi q + 3) \exp(\sin(2\pi q + 3))dt + \sigma dW_3, \end{cases} \quad (64)$$

where dW_i are independent Brownian motions. This is inspired by the so-called Kolmogorov flow [9] (see Eq.(66)). The Kolmogorov flow is obtained from the Arnold-Beltrami-Childress (ABC) flow with $A = B = C = 1$ and with cosines taken out. Behaviors of classic Kolmogorov flow will be discussed later.

In our numerical experiments, we choose $\Delta t_{ref} = 0.001$ and $N_{mc} = 6,400,000$ to solve the SDE (64) and compute the reference solution, i.e., the “exact” effective diffusivity. After some numerical tests, we find that the passive tracer model will enter a mixing stage if the computational time is set to be $T = 2400$. It takes about 56 hours to compute the reference solution on the server and the reference solution for the effective diffusivity is $D_{11} = 0.13106$.

In Fig. 1b, we plot the convergence results of the effective diffusivity using our method with respect to different time-step Δt . In addition, we show a fitted straight line with the slope 1.27, i.e., the convergence rate is about $(\Delta t)^{1.27}$. This numerical result also agrees with our error analysis.

5.2. Investigation of the diffusion enhancement phenomenon

We first investigate convection-enhanced diffusion phenomenon in the classical ABC flow with our symplectic stochastic integrators. The ABC flow is a three-dimensional incompressible velocity field which is an exact solution to the Euler’s equation. It is notable as a simple example of a fluid flow that can have chaotic trajectories. The particle is transported by the velocity field $(A \sin(r) + C \cos(q), B \sin(p) + A \cos(r), C \sin(q) + B \cos(p))$ and

perturbed by an additive noise. The associated passive tracer model reads

$$\begin{cases} dp = (A \sin(r) + C \cos(q))dt + \sigma dW_1, \\ dq = (B \sin(p) + A \cos(r))dt + \sigma dW_2, \\ dr = (C \sin(q) + B \cos(p))dt + \sigma dW_3, \end{cases} \quad (65)$$

where dW_i are independent Brownian motions. In Fig.2, we show the relation between D_{11}^E and D_0 . Recall that the parameter $D_0 = \sigma^2/2$. By setting $A = B = C = 1$, we recover the same phenomenon as the Fig.2 in [4], for $D_0 \in [10^{-3}, 10^{-1}]$ and can extend to $D_0 \in [10^{-5}, 10^{-4}]$; see Fig.2. At the same time, we can see that the Euler method failed when D_0 is small, which is also confirmed in [29]. The Fig.2 shows that the D_{11}^E of the ABC flow obtained by our symplectic method corresponds to upper-bound of (6), i.e. the maximal enhancement, $D_{11}^E \sim \mathcal{O}(1/D_0)$. This maximal enhancement phenomenon may be attributed to the ballistic orbits of the ABC flow, which was discussed in [20, 30].

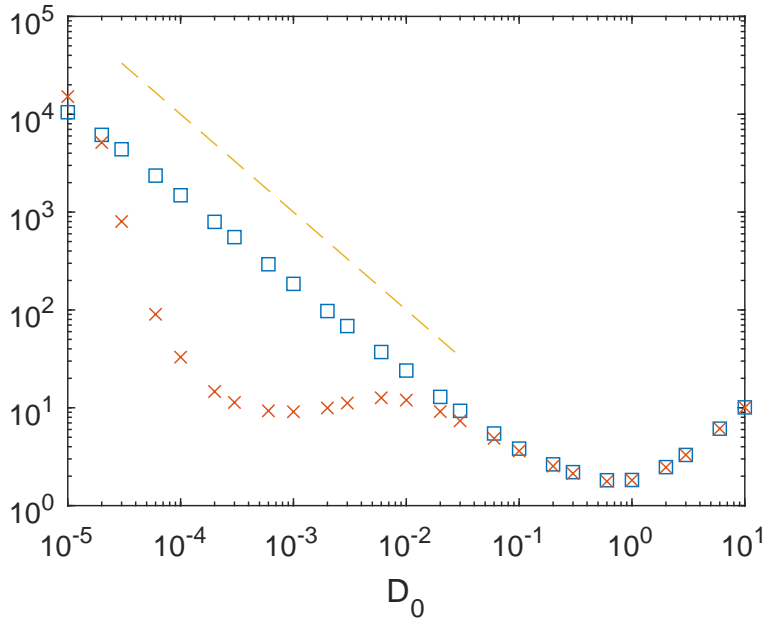
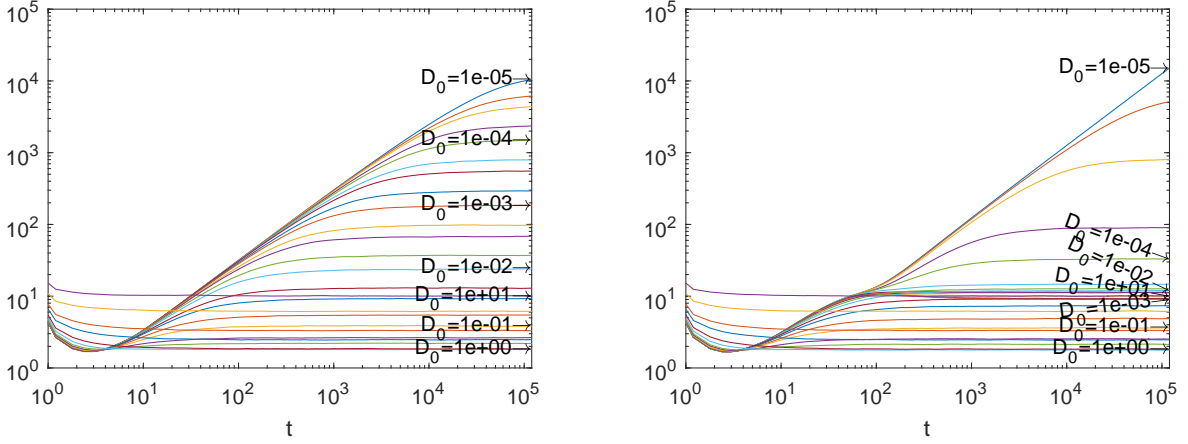


Figure 2: Convection-enhanced diffusion with maximal enhancement in ABC flow: \square for the symplectic scheme, \times for the Euler scheme, $--$ for reference line $y = \frac{1}{D_0}$.

From Fig.3a we can see that diffusing time, i.e., the time that $\langle \frac{p(t)^2}{2t} \rangle$ approaches a constant, increases as $\mathcal{O}(1/D_0)$ when $D_0 \rightarrow 0$ in the symplectic scheme. To the best of our knowledge, the $\mathcal{O}(1/D_0)$ scale of the diffusion time of the ABC flow is not known before. Moreover, Fig.3a shows that our numerical scheme is very robust in computing the effective diffusivity for the ABC flow. However, the Euler scheme gives a wrong result in Fig.3b since the time $\langle \frac{p(t)^2}{2t} \rangle$ approaching a constant does not agree with the expected diffusion time $\mathcal{O}(1/D_0)$. The statement that the Euler scheme will generate wrong results can also be found in the Fig.2.



(a) $\langle \frac{p(t)^2}{2t} \rangle$ of different D_0 in the symplectic scheme (b) $\langle \frac{p(t)^2}{2t} \rangle$ of different D_0 in the Euler scheme

Figure 3: Calculated D_{11}^E in the ABC flow along time via two different schemes

We point out that the error estimate in Theorem 4.7 is just an upper bound. Fig.4 shows that when D_0 is 10^{-3} , the convergence rate is about $\mathcal{O}(\Delta t^{1.42})$. It is very expensive to study the passive tracer model for the ABC flow since the diffusing time is extremely long. In our numerical test for the Fig.4, we choose $N_{mc} = 120,000$, $\Delta t = 0.001$, and $T = 12,000$. In this setting, the error of the Monte Carlo simulation cannot be avoided, so there is a small oscillation around the fitted slope.

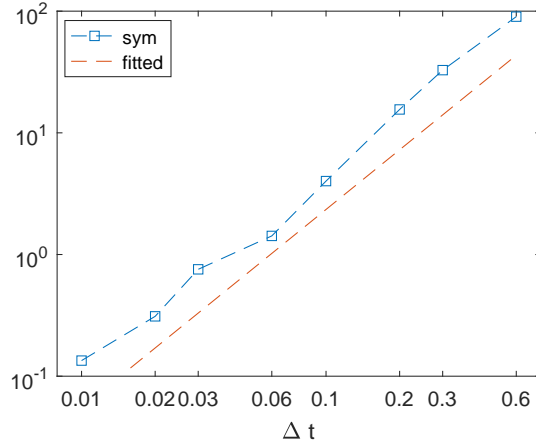


Figure 4: Error of D_{11}^E in the ABC flow, the dashed line with \square is for the symplectic scheme, and the slope of the fitted is ≈ 1.42 .

Finally, we investigate the diffusion enhancement phenomenon for another chaotic flow, i.e., the Kolmogorov flow. The associated passive tracer model reads,

$$\begin{cases} dp = \sin(r)dt + \sigma dW_1, \\ dq = \sin(p)dt + \sigma dW_2, \\ dr = \sin(q)dt + \sigma dW_3, \end{cases} \quad (66)$$

where dW_i are independent Brownian motions. In Fig.5, we show the relation between D_{11}^E and D_0 . For each D_0 , we use $N_{mc} = 120,000$ particles to solve the SDE (66) via the symplectic method and the Euler method with $\Delta t = 0.1$. The final computational time is $T = 12,000$ so that the particles are fully mixed for $D_0 \geq 10^{-6}$.

Under such setting, we find that the dependency of D_{11}^E on D_0 is quite different from the chaotic and stochastic flows that we have studied in [29] and from the foregoing ABC flow (maximal enhancement). The fitted slope within $D_0 \in [10^{-6}, 10^{-5}]$ is -0.13 , which indicates that $D_{11}^E \sim \mathcal{O}(1/D_0^{0.13})$. This can be called sub-maximal enhancement, which may be explained by the fact that the Kolmogorov flow is more chaotic than the ABC flow [9]. The chaotic trajectories in Kolmogorov flow enhance diffusion much less than channel like structures such as the ballistic orbits of ABC flows [20, 30]. More studies on the diffusion enhancement phenomenon of the ABC flow and the Kolmogorov flow, especially the time-dependent cases will be reported in our future work.

We also compare the performance of the symplectic scheme and Euler scheme in computing the effective diffusivity for the Kolmogorov flow. Specifically, we implement the symplectic scheme and Euler scheme with time step $\Delta t = 0.1$ and $\Delta t = 0.01$, respectively. In Fig.5, we find that (1) the symplectic scheme with $\Delta t = 0.1$ and $\Delta t = 0.01$ will give similar results in computing the effective diffusivity; (2) the symplectic scheme and the Euler scheme with $\Delta t = 0.01$ will give almost the same convergent results in computing the effective diffusivity, which provides evidence that our statement on the Kolmogorov flow (i.e., the sub-maximal enhancement phenomenon) is correct; (3) the Euler scheme with $\Delta t = 0.1$ gives wrong results but the symplectic scheme with $\Delta t = 0.1$ gives acceptable results, which provides evidence that the symplectic scheme is very robust in computing the effective diffusivity. In this example, the symplectic scheme approximately achieves a $10\times$ speedup over the Euler scheme.

Fig.6a and Fig.6b show different behaviors of the numerical effective diffusivity $\langle \frac{p(t)^2}{2t} \rangle$ obtained using the symplectic scheme and the Euler scheme with respect to computational time. Specifically, Fig.6a shows $T = 12000$ is quite enough for $D_0 \geq 10^{-6}$. And in Fig.6b, it seems that in Euler scheme, the diffusion time is much smaller. Our understanding is that the numerical diffusion in Euler scheme helps reach its own diffusion time earlier. In Fig.7, we also study the convergence rate of the symplectic scheme in computing the effective diffusivity for the Kolmogorov flow (66). We find that the convergence rate is $\mathcal{O}(\Delta t^{1.3043})$ in this example.

6. Conclusions

In this paper, we analyzed a robust numerical scheme to compute the effective diffusivity of passive tracer models, especially for the three-dimensional ABC flow and the Kolmogorov flow. Our scheme is based on the Lagrangian formulation of the passive tracer model, i.e., solving SDEs. We split the SDE problem into a deterministic sub-problem and a random perturbation, where the former is discretized using a symplectic-preserving scheme while the later is solved using the Milstein scheme. We provide a completely new error analysis for our numerical scheme that is based on the probabilistic approach, which gives a sharp and

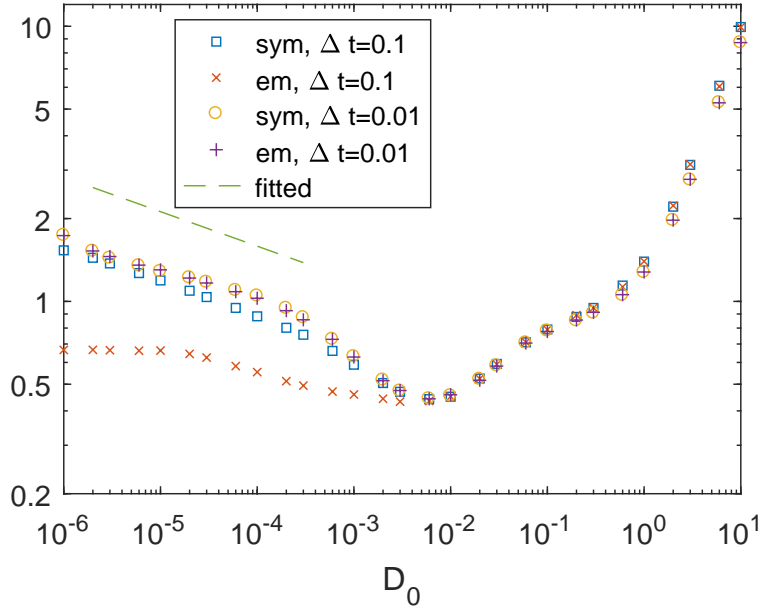
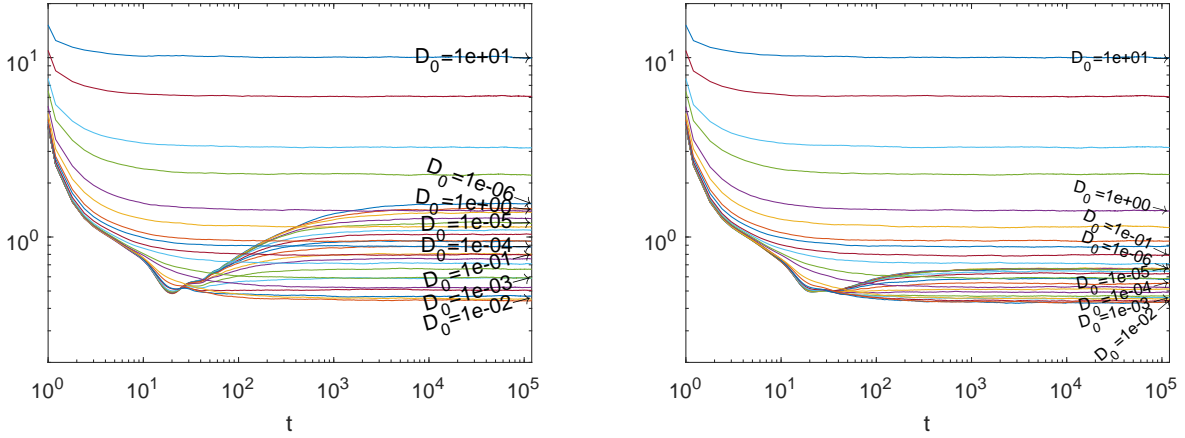


Figure 5: Convection-enhanced diffusion with sub-maximal enhancement in Kolmogorov flow. “sym” means the results for symplectic method and “em” means the results for Euler method. — means the fitted line for small D_0 with slope ≈ -0.13 .



(a) $\langle \frac{p(t)^2}{2t} \rangle$ of different D_0 using the symplectic scheme

(b) $\langle \frac{p(t)^2}{2t} \rangle$ of different D_0 in Euler scheme

Figure 6: Calculated D_{11}^E in the Kolmogorov flow via two different schemes.

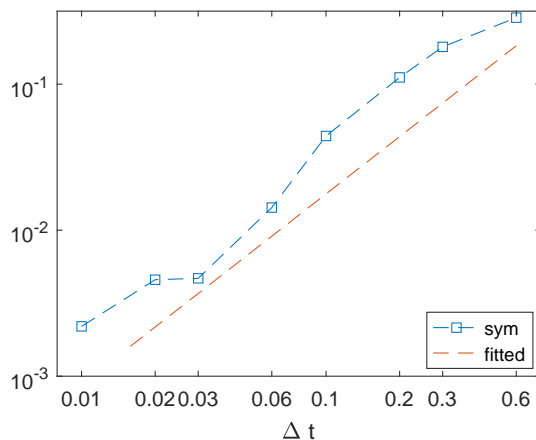


Figure 7: Error of D_{11}^E in the Kolmogorov flow. The slope of the fitted line is ≈ 1.30 .

uniform in time error estimate for the numerical solution of the effective diffusivity. Finally, we present numerical experiments to demonstrate the accuracy of the proposed method for several typical chaotic flow problems of physical interests, including the Arnold-Beltrami-Childress (ABC) flow and the Kolmogorov flow. We observed the maximal enhancement phenomenon in the ABC flows model and the sub-maximal enhancement phenomenon in the Kolmogorov flow, respectively.

There are two directions we plan to explore in our future work. First, we shall extend the probabilistic approach to provide sharp convergence analysis in computing effective diffusivity for time-dependent chaotic flows, such as time-dependent ABC flows. In addition, we shall investigate the convection-enhanced diffusion phenomenon for general spatial-temporal stochastic flows [16] and develop convergence analysis for the corresponding numerical methods.

Acknowledgements

The research of Z. Wang is partially supported by the Hong Kong PhD Fellowship Scheme. The research of J. Xin is partially supported by NSF grants DMS-1211179 and DMS-1522383. The research of Z. Zhang is supported by Hong Kong RGC grants (Projects 27300616, 17300817, and 17300318), National Natural Science Foundation of China (Project 11601457), Seed Funding Programme for Basic Research (HKU), an RAE Improvement Fund from the Faculty of Science (HKU), and the Hung Hing Ying Physical Sciences Research Fund (HKU). The computations were performed using the HKU ITS research computing facilities that are supported in part by the Hong Kong UGC Special Equipment Grant (SEG HKU09).

References

References

- [1] B. Afkham and J. Hesthaven. Structure preserving model reduction of parametric hamiltonian systems. *SIAM Journal on Scientific Computing*, 39(6):A2616–A2644, 2017.

- [2] G. Ben Arous and H. Owhadi. Multiscale homogenization with bounded ratios and anomalous slow diffusion. *Communications on Pure and Applied Mathematics*, 56(1):80–113, 2003.
- [3] A. Bensoussan, J. L. Lions, and G. Papanicolaou. *Asymptotic analysis for periodic structures*, volume 374. American Mathematical Soc., 2011.
- [4] L. Biferale, A. Crisanti, M. Vergassola, and A. Vulpiani. Eddy diffusivities in scalar transport. *Phys. Fluids*, 7:2725–2734, 1995.
- [5] R. Carmona and L. Xu. Homogenization for time-dependent two-dimensional incompressible Gaussian flows. *The Annals of Applied Probability*, 7(1):265–279, 1997.
- [6] A. Fannjiang and G. Papanicolaou. Convection-enhanced diffusion for periodic flows. *SIAM J Appl. Math.*, 54:333–408, 1994.
- [7] A. Fannjiang and G. Papanicolaou. Convection-enhanced diffusion for random flows. *J. Stat. Phys.*, 88:1033–1076, 1997.
- [8] K. Feng and Z. Shang. Volume-preserving algorithms for source-free dynamical systems. *Numerische Mathematik*, 71(4):451–463, 1995.
- [9] D. Galloway and M. Proctor. Numerical calculations of fast dynamos in smooth velocity fields with realistic diffusion. *Nature*, 356(6371):691, 1992.
- [10] J. Garnier. Homogenization in a periodic and time-dependent potential. *SIAM Journal on Applied Mathematics*, 57(1):95–111, 1997.
- [11] R. Gilmore. Baker-Campbell-Hausdorff formulas. *Journal of Mathematical Physics*, 15(12):2090–2092, 1974.
- [12] E. Hairer, C. Lubich, and G. Wanner. *Geometric numerical integration: structure-preserving algorithms for ordinary differential equations*. Springer Science and Business Media, 2006.
- [13] J. Hong, H. Liu, and G. Sun. The multi-symplecticity of partitioned runge-kutta methods for hamiltonian pdes. *Mathematics of computation*, 75(253):167–181, 2006.
- [14] V. V. Jikov, S. Kozlov, and O. A. Oleinik. *Homogenization of Differential Operators and Integral Functionals*. Springer, Berlin, 1994.
- [15] N. V. Krylov. *Lectures on elliptic and parabolic equations in Hölder spaces*. Graduate studies in mathematics.
- [16] C. Landim, S. Olla, and H. T. Yau. Convection–diffusion equation with space–time ergodic random flow. *Probability theory and related fields*, 112(2):203–220, 1998.

- [17] Y. Liu, J. Xin, and Y. Yu. Asymptotics for turbulent flame speeds of the viscous G-equation enhanced by cellular and shear flows. *Arch. Rational Mech. Anal.*, 202:461–492, 2011.
- [18] J. Lyu, J. Xin, and Y. Yu. Computing residual diffusivity by adaptive basis learning via spectral method. *Numerical Mathematics: Theory, Methods and Applications*, 10(2):351–372, 2017.
- [19] A. J. Majda and P. R. Kramer. Simplified models for turbulent diffusion: theory, numerical modelling, and physical phenomena. *Phys. Rep.*, 314:237–574, 1999.
- [20] T. McMillen, J. Xin, Y. F. Yu, and A. Zlatos. Ballistic orbits and front speed enhancement for abc flows. *SIAM Journal on Applied Dynamical Systems*, 15(3):1753–1782, 2016.
- [21] I. Mezić, J. F. Brady, and S. Wiggins. Maximal effective diffusivity for time-periodic incompressible fluid flows. *SIAM Journal on Applied Mathematics*, 56(1):40–56, 1996.
- [22] G. Milstein, Y. Repin, and M. Tretyakov. Symplectic integration of Hamiltonian systems with additive noise. *SIAM J. Numer. Anal.*, 39:2066–2088, 2002.
- [23] B. Oksendal. *Stochastic Differential Equations: an introduction with applications*. Springer Science and Business Media, 2013.
- [24] G. Pavliotis and A. Stuart. Periodic homogenization for inertial particles. *Physica D*, 204:161–187, 2005.
- [25] G. Pavliotis and A. Stuart. Homogenization for inertial particles in a random flow. *Commun Math Sci.*, 5:507–531, 2007.
- [26] G. Pavliotis and A. Stuart. *Multiscale methods: averaging and homogenization*. Springer Science and Business Media, 2008.
- [27] G. Pavliotis, A. Stuart, and K. Zygalakis. Calculating effective diffusivities in the limit of vanishing molecular diffusion. *J. Comput. Phys.*, 228:1030–1055, 2009.
- [28] G. Strang. On the construction and comparison of difference schemes. *SIAM J. Numer. Anal.*, 5:506–517, 1968.
- [29] Z. J. Wang, J. Xin, and Z. W. Zhang. Computing effective diffusivity of chaotic and stochastic flows using structure-preserving schemes. *SIAM Journal on Numerical Analysis*, 56(4):2322–2344, 2018.
- [30] J. Xin, Y. Yu, and A. Zlatos. Periodic orbits of the abc flow with $a = b = c = 1$. *SIAM Journal on Mathematical Analysis*, 48(6):4087–4093, 2016.
- [31] P. Zu, L. Chen, and J. Xin. A computational study of residual KPP front speeds in time-periodic cellular flows in the small diffusion limit. *Physica D*, 311:37–44, 2015.